



## Synthetic Flavonoids, Aminoisoflavones: Interaction and Reactivity with Metal-Free and Metal-Associated Amyloid- $\beta$ Species

Journal:	<i>Chemical Science</i>
Manuscript ID:	SC-EDG-05-2014-001531.R1
Article Type:	Edge Article
Date Submitted by the Author:	08-Jul-2014
Complete List of Authors:	<p>DeToma, Alaina; University of Michigan, Dept. of Chemistry          Krishnamoorthy, Janarthanan; University of Michigan,          Nam, Younwoo; Ulsan National Institute of Science and Technology,          Chemistry,          Lee, Hyuck Jin; University of Michigan, Chemistry          Brender, Jeffrey; University of Michigan, Chemistry;          Kochi, Akiko; University of Michigan,          Lee, Dongkuk; Seoul National University of Science and Technology, Fine          Chemistry          Onnis, V; University of Cagliari,          Congiu, C; University of Cagliari,          Manfredini, Stefano; University of Ferrara,          Vertuani, Silvia; University of Ferrara,          balboni, gianfranco; University, Dipartimento di Scienze della Vita e          dell'Ambiente          Ramamoorthy, A.; University of Michigan, Dept. of Chemistry          Lim, Mi Hee; Ulsan National Institute of Science and Technology,          Chemistry; University of Michigan, Life Sciences Institute</p>

## ARTICLE

# Synthetic Flavonoids, Aminoisoflavones: Interaction and Reactivity with Metal-Free and Metal-Associated Amyloid- $\beta$ Species

Cite this: DOI: 10.1039/x0xx00000x

Received 00th XXX 2014,  
Accepted 00th XXX 2014

DOI: 10.1039/x0xx00000x

www.rsc.org/

Alaina S. DeToma,<sup>1,§</sup> Janarthanan Krishnamoorthy,<sup>1,2,§</sup> Younwoo Nam,<sup>3,4,5</sup> Hyuck Jin Lee,<sup>1,5</sup> Jeffrey R. Brender,<sup>1,2</sup> Akiko Kochi,<sup>1,5</sup> Dongkuk Lee,<sup>4</sup> Valentina Onnis,<sup>6</sup> Cenzo Congiu,<sup>6</sup> Stefano Manfredini,<sup>7</sup> Silvia Vertuani,<sup>7</sup> Gianfranco Balboni,<sup>6,\*</sup> Ayyalusamy Ramamoorthy,<sup>1,2,\*</sup> and Mi Hee Lim<sup>3,5,\*</sup>

Metal ion homeostasis in conjunction with amyloid- $\beta$  (A $\beta$ ) aggregation in the brain has been implicated in Alzheimer's disease (AD) pathogenesis. To uncover the interplay between metal ions and A $\beta$  peptides, synthetic, multifunctional small molecules have been employed to modulate A $\beta$  aggregation *in vitro*. Naturally occurring flavonoids have emerged as a valuable class of compounds for this purpose due to their ability to modulate both metal-free and metal-induced A $\beta$  aggregation. Although, flavonoids have shown anti-amyloidogenic effects, the structural moieties of flavonoids responsible for such reactivity have not been fully identified. In order to understand the structure-interaction-reactivity relationship within the flavonoid family for metal-free and metal-associated A $\beta$ , we designed, synthesized, and characterized a set of isoflavone derivatives, aminoisoflavones (1-4), that displayed reactivity (*i.e.*, modulation of A $\beta$  aggregation) *in vitro*. NMR studies revealed a potential binding site for aminoisoflavones between the N-terminal loop and central helix on prefibrillar A $\beta$  different from the non-specific binding observed for other flavonoids. The absence or presence of the catechol group differentiated the binding affinities and enthalpy/entropy balance between aminoisoflavones and A $\beta$ . Furthermore, having a catechol group influenced the binding mode with fibrillar A $\beta$ . Inclusion of additional substituents moderately tuned the impact of aminoisoflavones on A $\beta$  aggregation. Overall, through these studies, we obtained valuable insights on the requirements for parity among metal chelation, intermolecular interactions, and substituent variation for A $\beta$  interaction.

## Introduction

Alzheimer's disease (AD) is rapidly becoming one of the most prominent public health concerns worldwide, especially due to the present lack of a curative treatment.<sup>1</sup> AD is commonly classified as a protein misfolding disease due to the observation of proteinaceous aggregates in diseased brain tissue, including senile plaques and neurofibrillary tangles.<sup>1b-e,2</sup> The primary components of the senile plaques are aggregated forms of amyloid- $\beta$  (A $\beta$ ) peptides.<sup>1b-e,3</sup> Self-association of monomeric A $\beta$  into various amyloid assemblies produces neurotoxic species, leading to AD pathogenesis;<sup>4</sup> however, plaques can have a heterogeneous composition, with other components identified in the deposits. For example, metal ions have been found in association with the plaques and could be linked to neurotoxicity in AD.<sup>1d,1e,2c,5</sup>

Cu(I/II), Zn(II), and more recently Fe(II) have been shown to bind to A $\beta$  peptides *in vitro*.<sup>1b-e,2c,5e,5f,6,7</sup> Consequently, Cu(II)- and Zn(II)-bound A $\beta$  peptides have been found to aggregate more rapidly than their metal-free counterparts.<sup>8</sup> It has also been proposed that redox active metal ions, such as Cu(I/II), bound to A $\beta$  could participate in redox cycling, leading to an overproduction of reactive oxygen species (ROS) and, subsequently, elevated oxidative stress.<sup>5c,5d,9</sup> As metal binding to A $\beta$  may have multiple potential

consequences, consideration of the direct interaction between these metal ions and A $\beta$  peptides as a pathological factor is warranted; however, little evidence has been accumulated to clarify the involvement of metal-associated A $\beta$  (metal-A $\beta$ ) species *in vivo* and their contribution to AD.

In an attempt to explore the connection between metal-A $\beta$  species and AD, employing small molecules as chemical tools may be useful. For this purpose, there have been increasing efforts to probe Cu(II)-A $\beta$  and Zn(II)-A $\beta$  *in vitro* using compounds with specific structural moieties for simultaneous interaction with metal ions and A $\beta$  (*i.e.*, bifunctionality).<sup>1b,1c,10</sup> The majority of molecules have been designed by direct modification of known A $\beta$  plaque imaging agents.<sup>10a-c,11</sup> In the incorporation design approach, heteroatoms for metal chelation are directly installed into the imaging agent framework.<sup>10,11</sup> This design strategy affords several advantages for future applications, including careful selection of moieties that could facilitate brain uptake and appropriate tuning of metal binding affinity to avoid systemic metal chelation and disruption of metal ion homeostasis in the brain.<sup>1b,10a,10b</sup> Although several compounds with bifunctionality have provided useful insights into the reactivity of metal-A $\beta$ , there remains much to be understood about these molecules' functions at the molecular level and the impact of their structural features on interaction and reactivity with metal-free and metal-A $\beta$  species. Rational screening

or selection of natural products has identified flavonoids as a source of chemical structures suitable for such investigation and modification.<sup>12</sup> Flavonoids are plant-derived compounds that have been studied in models of inflammation, cancer, oxidative stress, and dementia.<sup>13</sup> Initially, myricetin (Fig. 1a) was found to modulate metal-mediated A $\beta$  aggregation and neurotoxicity *in vitro* due to its metal chelation and A $\beta$  interaction properties.<sup>12a</sup> More recently, the influence of (-)-epigallocatechin-3-gallate (EGCG, Fig. 1a) on both metal-free and metal-induced A $\beta$  aggregation was characterized in detail at the molecular level.<sup>12b</sup> EGCG bound to metal-A $\beta$  was able to alter A $\beta$  conformation; off-pathway A $\beta$  aggregation occurred leading to amorphous A $\beta$  aggregates.<sup>12b,14</sup> This outcome represents an additional path by which the formation of toxic oligomeric A $\beta$  intermediates may be circumvented. In order to reconcile the previously reported findings using myricetin and EGCG with the rational design approach, it would be worthwhile to identify the essential structural moieties within a flavonoid framework required to target metal-free and metal-associated A $\beta$  species and modulate their reactivity, which will offer small molecule candidates as chemical tools for studying A $\beta$  and metal-A $\beta$  species.

Herein, we report the design and preparation of simple flavonoids derivatives, aminoisoflavones (**1-4**, Fig. 1b), with the intention to merge the qualities attained from rational-based design strategy into the isoflavone framework, which are known to contain auspicious biological characteristics toward AD (*vide infra*),<sup>13a,15</sup> along with detailed evaluation of their Cu(II), Zn(II), and A $\beta$  interaction properties for understanding their ability to regulate metal-free and metal-induced A $\beta$  aggregation. Our overall results and observations demonstrate that deconstruction of naturally occurring flavonoids for redesign with selective inclusion of only a few functional groups is sufficient to effectively target metal ions, A $\beta$ , and metal-A $\beta$  and to subsequently influence their reactivity (*i.e.*, modulation of A $\beta$  aggregation) *in vitro*. Moreover, structural modification of the isoflavone framework, chosen for its synthetically friendly scaffold, does not diminish its innate beneficial traits toward AD-related reactivity. Using our aminoisoflavone derivatives, the foundation of a structure-interaction-reactivity relationship for flavonoids toward metal-free and metal-associated A $\beta$  is strengthened by detailed characterization of their properties at the molecular level.

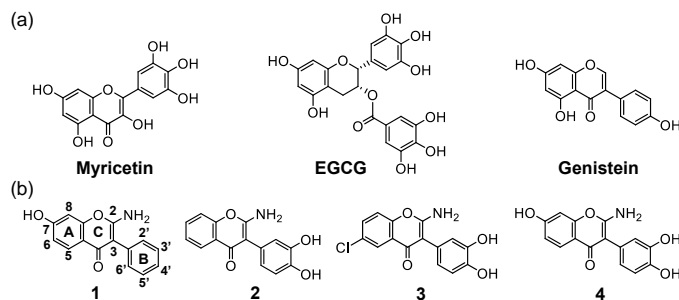
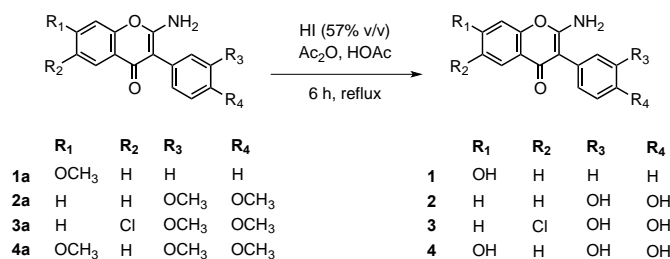


**Fig. 1.** Chemical structures of (a) naturally occurring flavonoids (myricetin, EGCG, and genistein) and (b) synthetic aminoisoflavones (**1-4**). (a) Left to right: Myricetin, 3,5,7-trihydroxy-2-(3,4,5-trihydroxyphenyl)-4H-chromen-4-one; EGCG, (-)-epigallocatechin-3-gallate or (2R,3R)-5,7-dihydroxy-2-(3,4,5-trihydroxyphenyl)chroman-3-yl 3,4,5-trihydroxybenzoate; genistein, 5,7-dihydroxy-3-(4-hydroxyphenyl)-4H-chromen-4-one. (b) Left to right: **1**, 2-amino-7-hydroxy-3-phenyl-4H-chromen-4-one; **2**, 2-amino-3-(3,4-dihydroxyphenyl)-4H-chromen-4-one; **3**, 2-amino-6-chloro-3-(3,4-dihydroxyphenyl)-4H-chromen-4-one; **4**, 2-amino-3-(3,4-dihydroxyphenyl)-7-hydroxy-4H-chromen-4-one.

## Results and Discussion

**Design and Synthesis of Aminoisoflavone Derivatives.** In search of small molecules to interrogate the relationship between metal ions and A $\beta$  species, selection of naturally occurring flavonoids has offered a new avenue for chemical tool development due to their multiple targeting capabilities, which may include various enzymes and ROS.<sup>12,16</sup> Recognizing that certain structural moieties are common to natural flavonoids (*e.g.*, catechol group; potentially for metal binding), a new family of synthetic flavonoids, aminoisoflavones (**1-4**, Fig. 1b) with tractable structural modifications were designed and prepared. Although the coordination chemistry of catechol and its corresponding metal complexes is well known,<sup>17</sup> knowledge of its role in flavonoid derivatives for targeting and modulating metal-free and metal-induced A $\beta$  aggregation has received little attention. Additionally, incorporation of an amine functionality (*e.g.*, NH<sub>2</sub>) could be used to gauge the tolerance of the framework to unnatural substituents,<sup>18</sup> which might be useful for tuning the metal binding and/or A $\beta$  interaction properties by rational structure-based modifications in later stages.

### Scheme 1. Synthetic route to aminoisoflavones (**1-4**)



The aminoisoflavones are derived from the structures of soy isoflavones, such as genistein (Fig. 1a), which are known to have multiple biological effects, and they have been employed as A $\beta$  aggregation inhibitors and as neuroprotective molecules.<sup>15</sup> Synthetic aminoisoflavone derivatives have been demonstrated previously to have inhibitory activity against various isoforms of human carbonic anhydrase (hCAI and hCAII),<sup>19</sup> a metalloenzyme that has been occasionally linked to AD.<sup>20</sup> Thus, we were curious to know whether the family of compounds could target and modulate another aspect of AD-related reactivity. The design of the new aminoisoflavones **1-4** (Fig. 1b) involves the *o*-dihydroxy moiety (*i.e.*, catechol) for metal chelation in **2**, **3**, and **4** and substituents, such as OH or Cl, in the A ring to modify the electronics or sterics of the molecules to influence their reactivity with A $\beta$  or metal-A $\beta$  (*vide infra*). Compound **1** was prepared as an analogue of **4** that lacks the catechol group for comparison of interaction and reactivity with metal ions, A $\beta$ , and metal-A $\beta$ . The design further employs an unnatural substituent, a primary amine, in the 2 position of the C ring within the core framework of the isoflavone, which may be beneficial for improving solubility compared to naturally occurring flavonoids (Fig. 1).<sup>18</sup> The inclusion of the amine group is also related to the design of A $\beta$  plaque imaging agents and multifunctional small molecules that have used amine derivatives to interact with the peptide.<sup>11a-d,11i,21</sup> Among them, the dimethylamino functionality has been commonly used; however, the reported derivatives containing the primary amine can also enable interaction with A $\beta$ .<sup>11d</sup> The aminoisoflavones (**1-4**)

presented here are synthesized by acidic cleavage of the

aggregates were shown in previous reports;<sup>12b,14,23,24</sup> similarly, TEM

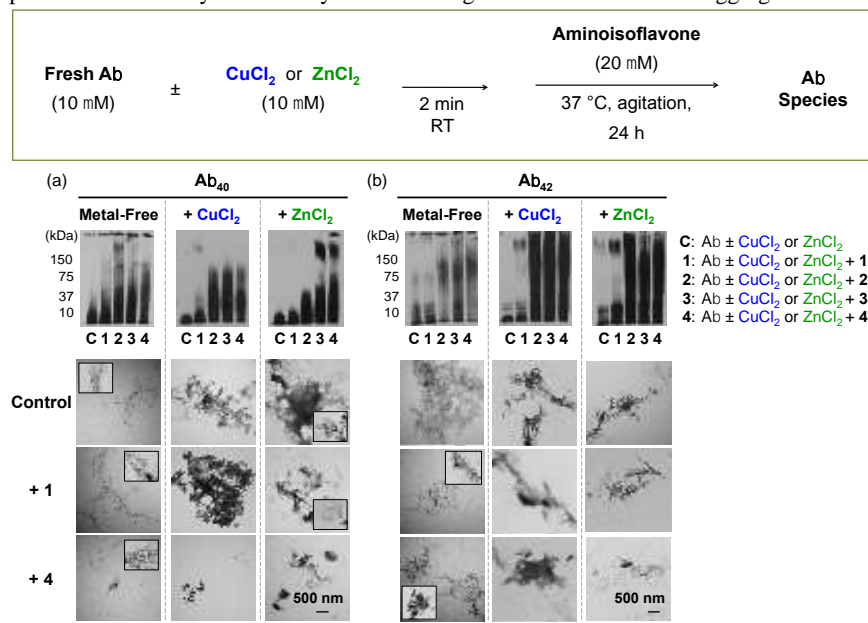


**Fig. 2.** Investigation of the ability of aminoisoflavones (**1-4**) to modulate the formation of metal-free and metal-induced Aβ<sub>40</sub> and Aβ<sub>42</sub> aggregates. Top: Scheme of the inhibition experiment. Middle: Analysis of the samples including (a) Aβ<sub>40</sub> and (b) Aβ<sub>42</sub> by gel electrophoresis followed by Western blot (6E10). Lanes: (C) Aβ ± CuCl<sub>2</sub> or ZnCl<sub>2</sub> (C = control), (1) C + 1; (2) C + 2; (3) C + 3; (4) C + 4. Bottom: TEM images of samples with **1** or **4** for (a) Aβ<sub>40</sub> and (b) Aβ<sub>42</sub>. Experimental conditions: [Aβ<sub>40</sub> or Aβ<sub>42</sub>] = 10 μM; [CuCl<sub>2</sub> or ZnCl<sub>2</sub>] = 10 μM; [aminoisoflavone] = 20 μM; 1% v/v DMSO; 20 mM HEPES, pH 7.4, 150 mM NaCl; 24 h; 37 °C; agitation.

methoxylated aminoisoflavone precursors,<sup>16b</sup> and they were obtained in relatively high yield (76-86%) (Scheme 1). Thus, the multiple structural aspects of these aminoisoflavones, including the isoflavone framework, the catechol motif, and the primary amine, make them attractive candidates for detailed characterization of their chemical properties, subsequent influence on metal-free and metal-induced Aβ aggregation *in vitro*.

**Aβ Aggregation in the Absence and Presence of Aminoisoflavones.** The extent to which the aminoisoflavones could control Aβ aggregation (inhibition experiment; Fig. 2) or alter preformed Aβ aggregates (disaggregation experiment; Fig. S1) in the absence and presence of Cu(II) and Zn(II) was investigated.<sup>10g-1,10a,10p,12a,12b,22</sup> For both studies, gel electrophoresis with Western blot was used to visualize the molecular weight (MW) distribution of the resulting Aβ species and transmission electron microscopy (TEM) was employed to detect changes to peptide morphology.

In the inhibition experiment, differences in reactivity of compounds were observed toward both metal-free and metal-induced Aβ aggregation (Fig. 2). Reactivity of compounds is inferred by the ability of the compound to modulate the peptide aggregation pathway; aiming to generate Aβ species with a wide distribution of MW which are soluble to penetrate the gel matrix. All of the aminoisoflavones were able to modulate metal-free Aβ<sub>40</sub> aggregation as evidenced by the range of various-sized Aβ species visualized (Fig. 2a, lanes 1-4) in comparison to compound-free Aβ (lane C). In the presence of Cu(II) or Zn(II), however, varying degrees of compounds' ability to control metal-triggered Aβ<sub>40</sub> aggregation were observed. Cu(II)- or Zn(II)-mediated Aβ<sub>40</sub> aggregation was influenced by catechol containing compounds; **2**, **3**, and **4**, but not by **1**, generating Aβ<sub>40</sub> species having MW ≤ 75 kDa (lanes 2-4), which may indicate the redirection of Aβ aggregation as previously described for flavonoids.<sup>12b,14,23,24</sup> Fewer high MW gel-permeable aggregates were detected with **2** in comparison to that of **3** and **4** (lanes 2-4), which may represent a modest effect from the inclusion of the additional substituents (*i.e.*, Cl, OH) that are present in the A ring for **3** and **4** on peptide aggregation relative to the unsubstituted analogue **2** (Figure 1b). Unstructured, amorphous Aβ

images of Cu(II)- and Zn(II)-added Aβ samples treated with **4** revealed smaller-sized, amorphous species, while larger Aβ aggregates were observed with compound-untreated metal-Aβ samples (Fig. 2). In contrast, **4**-added metal-free Aβ samples displayed structured Aβ aggregates similar to those of compound-free Aβ<sub>40</sub>. In addition, minimal morphological changes were exhibited upon treatment of **1** in both metal-free and metal-treated conditions, suggesting that **1** may interact with metal-free and metal-associated Aβ species differently from **4**.

Furthermore, in order to understand structural moieties that could play a role in the control of Aβ aggregation, the reactivity of catechol (a metal binding site in **2-4**) and a mixture of **1** (flavonoid only) and catechol with metal-free and metal-associated Aβ<sub>40</sub> was investigated (Fig. S2). In metal-free conditions, some reactivity toward Aβ<sub>40</sub> was only observed for **1** or a mixture of **1** and catechol (Fig. S2, lanes 2 and 4), implying that the structural framework of **1**, and not catechol, may be important for metal-free Aβ<sub>40</sub> aggregation. In the case of metal-induced Aβ<sub>40</sub> aggregation, no reactivity was indicated with **1** (lane 2), while noticeable reactivity was displayed with metal-Aβ treated with catechol or a mixture of **1** and catechol (lanes 3 and 4). Moreover, the reactivity of the mixture of **1** and catechol was more distinguishable toward Cu(II)-Aβ<sub>40</sub>, in comparison to that of catechol, similar to that shown by **2-4**. On the other hand, Zn(II)-induced Aβ<sub>40</sub> aggregation was less modulated by catechol and a mixture of **1** and catechol than **2-4**. These observations suggest that the catechol moiety and **1** in the structural framework of **2-4** could be important for interaction with metal-Aβ<sub>40</sub> and metal-free Aβ<sub>40</sub> species, respectively; however, the ability of **2-4** to control metal-free and metal-induced Aβ<sub>40</sub> aggregation is driven by their overall structure (not by individual structural components).

It is also relevant to consider the reactivity of these ligands with Aβ<sub>42</sub>, which has been suggested to primarily compose the senile plaques and found to aggregate *via* different intermediates in comparison to Aβ<sub>40</sub>.<sup>1e,2b,3b,25</sup> Overall patterns observed for Aβ<sub>42</sub> were similar to those for Aβ<sub>40</sub> in the inhibition experiment (*vide supra*; Fig. 2). Metal-free Aβ<sub>42</sub> aggregation was modestly influenced by **2**,

**3**, and **4**, with a lesser extent with **1** (Fig. 2b, lanes 1-4). In samples containing metal ions, **2**, **3**, and **4** showed analogous greater reactivity, over metal-free conditions, visualized by the darker intensity of gel bands suggesting that all three compounds may alter metal-induced A $\beta$ <sub>42</sub> aggregation in a similar fashion (lanes 2-4). Noticeably less reactivity was displayed with **1** in either metal-free or metal-triggered A $\beta$ <sub>42</sub> aggregation. From the TEM results, mixtures of large, amorphous A $\beta$ <sub>42</sub> species were observed in metal-free and metal-treated conditions upon the treatment of **4** in comparison to compound-untreated metal-free or metal-A $\beta$  which displayed structured A $\beta$ <sub>42</sub> aggregates.

The aminoisoflavones were also evaluated on their ability to transform preformed metal-free or metal-associated A $\beta$ <sub>40</sub> or A $\beta$ <sub>42</sub> aggregates (Fig. S1). Overall, the pattern of compound reactivity observed in the disaggregation experiments were similar to those of the inhibition experiment. In samples containing A $\beta$ , metal ions, and **2**, **3**, or **4** (lanes 2-4), different distribution patterns was exhibited in comparison to those of compound-free conditions (lanes C). In contrast to inhibition results, minimal reactivity was observed upon the treatment of **1**, **2**, **3**, or **4** to metal-free A $\beta$ <sub>40</sub> aggregates (lanes 1-4). Different from **1**, metal chelation *via* the catechol moiety in **2**, **3**, and **4**, could likely play a role in redirecting preformed metal-A $\beta$ <sub>42</sub> aggregates. The TEM results showed a mixture of different-sized amorphous A $\beta$  aggregates upon the treatment of **4** to either metal-free or metal-induced A $\beta$  species, while more structured A $\beta$  aggregates were present for compound-untreated samples in the same conditions (Fig. S1).

Furthermore, the methoxylated precursors of **1**, **2**, and **4** (*i.e.*, **1a**, **2a**, and **4a**, respectively; Scheme 1) were also studied in order to determine the potential role of the catechol moiety in the reactivity of aminoisoflavones toward metal-free/-induced A $\beta$  aggregation. As depicted in Fig. S3, very minimal effect of **1a**, **2a** or **4a** was observed only with Cu(II)-A $\beta$ <sub>40</sub> in both inhibition and disaggregation experiments. In all scenarios, **1a**, **2a** or **4a** did not affect metal-free or Zn(II)-mediated A $\beta$ <sub>40/42</sub> aggregation. Taken together, our inhibition and disaggregation results reveal the scope of flavonoid derivatives that can be used to modulate metal-free and metal-induced A $\beta$  aggregation and validate the requirement for sufficient metal binding and A $\beta$  interaction properties to suitably influence this reactivity. The absence of metal chelation moiety, catechol, in **1** as well as **1a**, **2a** or **4a** hindered the modulation of metal-induced

A $\beta$ <sub>40/42</sub> aggregation, implying that the catechol moiety may be a key factor in the reactivity of aminoisoflavones with metal-A $\beta$  species. Moreover, additional substituents on the A ring (*i.e.*, Cl for **3** and OH for **4**) may also effect the modulation of A $\beta$  aggregation.

**Solution Speciation Studies of Aminoisoflavones.** The acidity constants ( $pK_a$ ) for the aminoisoflavones were determined by variable-pH spectrophotometric titrations ( $I = 0.1$  M, room temperature) following previously reported procedures (Fig. 3).<sup>10f,10h-1,10a,10p,26</sup> The primary amine common to all four aminoisoflavones was assigned to the most acidic  $pK_a$  values, consistent with the predicted values for these structures.<sup>27</sup> Deprotonation of the ammonium (RNH<sub>3</sub><sup>+</sup>) to the primary amine (RNH<sub>2</sub>) was represented by  $pK_a$  values of  $1.3 \pm 0.1$  for **1**,  $1.8 \pm 0.5$  for **2**,  $2.2 \pm 0.9$  for **3**, and  $1.5 \pm 0.4$  for **4**. With the exception of **1**, each of the structures contains the catechol moiety that had expected  $pK_a$  values of *ca.* 9 and 13 for the hydroxyl groups.<sup>17a-c</sup> The  $pK_a$  values for the catechol/catecholate equilibrium were  $8.9 \pm 0.2$  and  $12.3 \pm 0.4$  for **2**,  $8.9 \pm 0.3$  and  $11.7 \pm 0.2$  for **3**, and  $9.1 \pm 0.2$  and  $12.0 \pm 0.2$  for **4**, with the more basic  $pK_a$  value corresponding to deprotonation of the hydroxyl group in the *para* position.<sup>17a-c</sup> An additional  $pK_a$  value corresponding to deprotonation of the hydroxyl substituent on the A ring in **1** and **4** was  $7.9 \pm 0.1$  and  $5.8 \pm 0.3$ , respectively.

Based on these  $pK_a$  values, speciation diagrams were drawn to illustrate the fraction of ligand protonation states at each pH in solution. Each ligand would exist mainly in its fully deprotonated form above pH 12 (*i.e.*, L), and would have an overall negative charge. At pH 7.4, the dominant species is expected to be neutral for **1** (LH), **2** (LH<sub>2</sub>), and **3** (LH<sub>2</sub>), or monodeprotonated for **4** (LH<sub>2</sub>). For future applications of these molecules, neutral species would be favored for facilitating brain uptake *via* passive diffusion across the blood-brain barrier (BBB).<sup>28</sup> Furthermore, characterization of the species distribution could be valuable for rationalizing the metal/A $\beta$  binding properties for these molecules as described below.

**Metal Binding Studies.** The aminoisoflavones **2**, **3**, and **4** were designed to be capable of metal binding *via* a catechol group, similar to other polyphenols.<sup>12a,12b,29</sup> The catechol moiety is a prevalent ligand in biology, appearing in naturally occurring molecules, such as flavonoids, and in neurotransmitters (*e.g.*, dopamine, epinephrine).<sup>17b,30</sup> Known to be a strong metal chelator, the inclusion

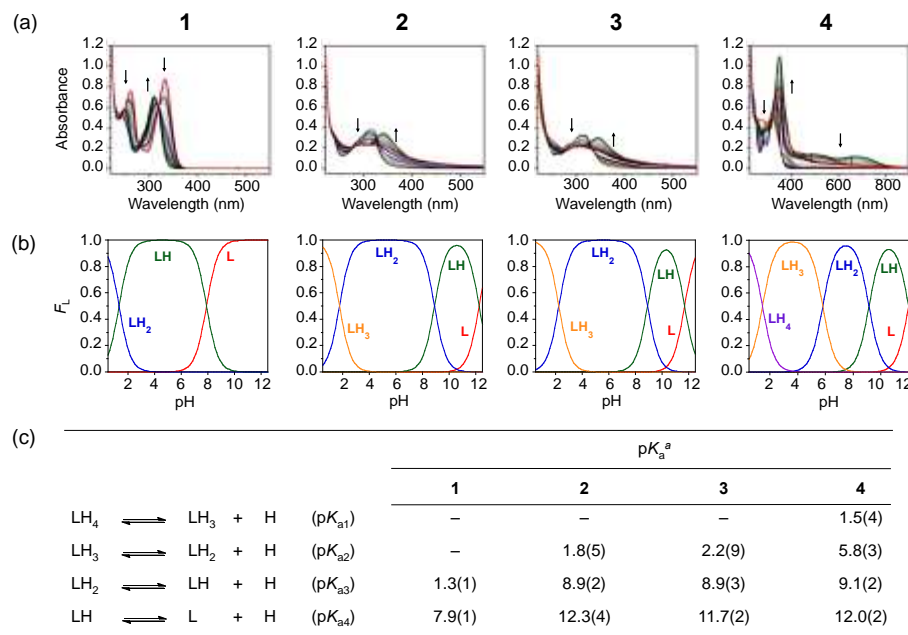


**Fig. 3.** Solution speciation studies of aminoisoflavones (**1-4**). (a) Variable-pH UV-Vis titration spectra and (b) solution speciation diagrams for **1-4** ( $F_L$  = fraction of species in solution). (c) Summary of solution equilibria and acidity constants. Experimental conditions: [**1** or **4**] = 30  $\mu$ M, [**2**] = 20  $\mu$ M, [**3**] = 15  $\mu$ M;  $I$  = 0.1 M NaCl; room temperature. Charges are omitted for clarity. <sup>a</sup> The error in the last digit is shown in parentheses.

of this functionality in the aminoisoflavone framework was anticipated to interact with metal ions surrounded by  $A\beta$  species.<sup>17b,17c,31</sup> Thus, the Cu(II) and Zn(II) binding properties of the aminoisoflavones were investigated initially by UV-Vis in the absence and presence of  $A\beta_{40}$  (Figs. S4-S6). More detailed Cu(II) binding properties were also characterized by variable-pH UV-Vis titrations. Upon incubation of the aminoisoflavones **2**, **3**, and **4** (20  $\mu$ M, 1% v/v DMSO) with  $CuCl_2$  in an aqueous buffered solution (20 mM HEPES, pH 7.4, 150 mM NaCl), differences in the optical spectrum of the free ligand were observed (Fig. S4). With 0.5 equiv of  $CuCl_2$ , new absorption features at ca. 480 nm were detected; additionally, prolonged incubation of the solution resulted in the appearance of a broad feature centered at ca. 800 nm.<sup>32</sup> Subsequent addition of  $CuCl_2$  enhanced the intensity of these peaks (Fig. S4). Note that the peak at ca. 800 nm was not observed from the solutions containing only the compounds, suggesting the involvement of Cu(II) in that optical feature. No noticeable changes in the optical spectra were observed with **1**, which lacks the catechol group (Fig. S4).

Zn(II) binding to the aminoisoflavones was also investigated by UV-Vis. It should be noted that the ligand concentration was increased to a ten-fold excess (*i.e.*, 100  $\mu$ M) relative to  $ZnCl_2$  (10  $\mu$ M) in order to detect an optical change upon metal binding (Fig. S5). Similar to the Cu(II) binding data, addition of Zn(II) had no effect on the spectrum of **1** (Fig. S5a). There were also no substantial changes for **3** with Zn(II); however, **2** and **4** showed new features in the UV-Vis spectra after ca. 12-24 h incubation. For **2**, an increase in the peak at ca. 285 nm and a shift to ca. 390 nm were observed (Fig. S5b). Similarly, **4** displayed a progressive bathochromic shift from ca. 320 nm to 350 nm over 24 h (Fig. S5d). These spectral variations could be indicative of partial deprotonation of the hydroxyl groups upon Zn(II) binding.<sup>30</sup> This partial ligand deprotonation might also cause a weak, broad feature around 800 nm that is similar to, but less intense than, that of the Cu(II) binding spectra.<sup>32</sup> This observation correlates to the Cu(II) speciation results at pH 7.4 detailed below, which suggests partial deprotonation of the catechol upon metal binding.<sup>17b,30</sup> Thus, deprotonation of **4** from  $LH_2$  to its  $LH$  form at Zn(II) binding to some extent.

To anticipate whether the aminoisoflavones might bind to metal ions in the presence of  $A\beta$ , UV-Vis studies were conducted with  $A\beta_{40}$ ,  $CuCl_2$ , and **4** (Fig. S6). The titration experiments were performed by two different means. First,  $A\beta_{40}$  (10  $\mu$ M) was incubated with  $CuCl_2$  for 5 min followed by **4**. Second,  $A\beta$  was added into the resulting solution generated after 5 min incubation of **4** (Fig. S6). Both cases were titrated to result in final  $[A\beta]:[CuCl_2]:[4]$  ratios of 1:0.5:2, 1:1:2, 1:2:2, or 1:4:2. The condition using a 1:1:2 ratio was representative of the concentrations used in the *in vitro* aggregation studies (*vide supra*), and the resulting Cu(II) binding spectra in the presence of  $A\beta$  were observed to have similar features as those acquired without peptide present from both titration experiments (Figs. S4 and S6). In the conditions using substoichiometric Cu(II) relative to  $A\beta$ , it was presumed that free Cu(II) in solution was minimal.<sup>1b-e,5f</sup> Incubation of **4** with the solution of  $A\beta$  and Cu(II) produced changes in the spectra, which was similarly observed when  $A\beta$  was introduced to a solution of **4** and Cu(II). Addition of **4** in Cu(II)-treated  $A\beta$  solution suggests potential Cu(II)-**4** complex formation; furthermore, presence of Cu(II)-**4** complex was still indicated upon  $A\beta$  treatment to the **4**-Cu(II)-added solution (Fig. S6), which implies that this compound may possibly compete with  $A\beta$  as a ligand for Cu(II).

Overall, these investigations demonstrate binding of the catechol-containing aminoisoflavone derivatives to Cu(II) and Zn(II). The samples of solutions containing Cu(II) and the

aminoisoflavones generated a unique optical feature, dominated by a low intensity transition bordering on the near-infrared (IR) region of the spectrum. This feature could correspond to changes in the electronic structure leading to a charge transfer process that populates a lower energy transition, as has been observed for different ligand frameworks.<sup>33</sup> Another possibility is that this feature represents a radical intermediate that was generated upon metal binding.<sup>17f,28,30</sup> It has been well established that deprotonated catechol participates in an equilibrium that involves the partially oxidized semiquinone and fully oxidized quinone.<sup>17f</sup> In the presence of divalent cations (*e.g.*, Cu(II)), this process might involve concomitant reduction of Cu(II) to Cu(I), while forming an oxidized ligand intermediate.<sup>17b,17f,35</sup> In a few cases, however, Cu(II)-semiquinone complexes have been reported; most of these complexes are relatively colorless ( $\epsilon_{800} \approx 500 \text{ M}^{-1}\text{cm}^{-1}$ ) and are paramagnetic.<sup>32,36</sup> To advance the understanding of the Cu(II) binding properties of the aminoisoflavones, **4** was used as a model ligand for further investigations.

Stability constants ( $\log\beta$ ) and the dissociation constants ( $K_d$ ) of Cu(II)-**4** complexes in solution (1:2 [Cu(II)]/[**4**],  $I = 0.1 \text{ M}$ , room temperature; pH 4-7) were determined by variable-pH UV-Vis titration experiments (Fig. 4).<sup>10f,10h,10j-1,10o,10p,26</sup> Based on the calculated  $\log\beta$  values, a solution speciation diagram was generated and indicated a mixture of Cu(II)-**4** complexes in 1:1 and 1:2 Cu(II)/ligand ratios. As depicted in Fig. 4, at pH 7.4, Cu(LH) existed relatively predominantly (ca. 80%; LH represents the monoprotonated form of **4** where the hydroxyl group in the *para* position of the B ring is protonated). There were additional species present at pH 7.4, such as  $Cu(LH)_2$  (ca. 18%) and  $Cu(LH_2)$  (ca. 2%). As indicated in Fig. 4, upon titration, the solution was mainly 1:1 complexes below pH 7 (*i.e.*,  $Cu(LH)$ ,  $Cu(LH_2)$ ,  $Cu(LH_3)$ ). From this model, **4** was found to have high binding affinity for Cu(II)

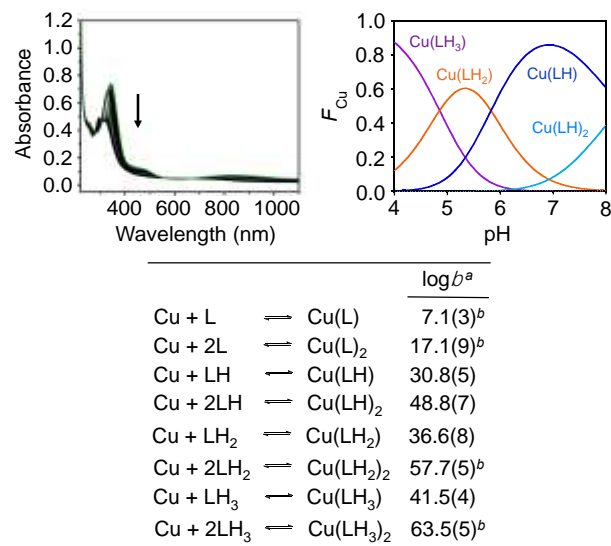


**Fig. 4.** Solution speciation studies of Cu(II)-**4** complexes. Top: Variable-pH UV-Vis titration spectra (left) and solution speciation diagram (right) for Cu(II)-**4** ( $F_{Cu}$  = fraction of species in solution relative to Cu(II)). Bottom: Summary of solution equilibria and stability constants ( $\log\beta$ ). Experimental conditions:  $[CuCl_2] = 15 \mu\text{M}$ ,  $[4] = 30 \mu\text{M}$ ; pH 8;  $I = 0.1 \text{ M}$  NaCl; room temperature. Charges are omitted for clarity. <sup>a</sup> The error in the last digit is shown in parentheses. <sup>b</sup> Cu(L), Cu(L)<sub>2</sub>, Cu(LH)<sub>2</sub>, and Cu(LH<sub>3</sub>)<sub>2</sub> were introduced in the calculation to provide the best fit to the data, but contributed a negligible amount to the overall solution speciation.

estimated based on the free Cu(II) concentration measured at a given pH (*i.e.*,  $pCu = -\log[Cu(II)_{\text{uncomplexed}}]$ ).<sup>10f,10h,10k,10l,10o,10p,26</sup> At pH 7.4, which was used for the *in vitro* experiments and is physiologically relevant, the  $pCu$  value for **4** was *ca.* 17, suggesting an estimated  $K_d$  for Cu(II)–**4** in the lower femtomolar range. The estimated  $K_d$  value for **4** to Cu(II) is slightly stronger than most reported  $K_d$  values for Cu(II)–A $\beta$  peptides (*i.e.*, nanomolar to picomolar) and could be used to rationalize the potential partial chelation of Cu(II) by **4** in the presence of A $\beta$  observed by UV-Vis (Fig. S6; *vide supra*).<sup>1b-e,5e,5f</sup> Along with the Cu(II) binding studies in the presence of A $\beta$  (Fig. S6), these data represent the possibility for **4** and other catechol-containing aminoisoflavone compounds (*e.g.*, **2**, **3**) could be competitive ligands for Cu(II) with A $\beta$ .

**Interaction of Aminoisoflavones with A $\beta$  Species.** The interaction between aminoisoflavones and A $\beta$  species in solution was investigated by isothermal titration calorimetry (ITC), NMR, and docking studies. ITC was first used to measure thermodynamic parameters for the interaction of A $\beta$  with **1**, **2**, and **4** (Table S1). Using a sequential binding model with one identical site to fit the data, these ligands were found to bind to A $\beta_{40}$  with *ca.* low mM affinity ( $K_A = 6.8 (\pm 3.0) \times 10^4$ ,  $7.9 (\pm 2.9) \times 10^3$ , and  $3.2 \pm (0.7) \times 10^3 \text{ M}^{-1}$  for **1**, **2**, and **4**, respectively) and with favorable values of Gibbs free energy ( $\Delta G = -27.3 (\pm 1.1)$ ,  $-22.2 (\pm 0.9)$ , and  $-19.9 (\pm 0.6) \text{ kJ/mol}$  for **1**, **2**, and **4**, respectively) (Table S1). Different peptide–ligand interactions, however, likely accounted for favorable binding. For **1**, which lacks the catechol moiety, entropic contributions ( $-T\Delta S = -38.7 (\pm 1.6) \text{ kJ/mol}$ ) were greater than enthalpic contributions ( $\Delta H = 11.3 (\pm 1.2) \text{ kJ/mol}$ ). Conversely, the enthalpic term for **4** is large and negative in magnitude ( $\Delta H = -116.3 (\pm 19.6) \text{ kJ/mol}$ ), while the contribution from entropy is unfavorable ( $-T\Delta S = 96.4 (\pm 19.6) \text{ kJ/mol}$ ). Similar to **4**, compound **2** showed favorable enthalpic ( $\Delta H = -59.1 (\pm 22.6) \text{ kJ/mol}$ ) and unfavorable entropic ( $-T\Delta S = 36.9 (\pm 22.6) \text{ kJ/mol}$ ) contributions (Table S1).

The thermodynamic parameters governing these peptide–small molecule interactions can be related to the variations in their chemical structures. Since **1** is distinguished from **2** or **4** by the absence of a catechol moiety for metal binding, it is reasonable to expect that these molecules may favor dissimilar interactions with the peptide. Compound **1** contains an unsubstituted phenyl ring, which might suggest that their interactions are mainly driven by hydrophobic interaction with the peptide; these types of interactions usually translate to an increase in the entropy as measured by ITC.<sup>37</sup> On the other hand, **4** would potentially facilitate the formation of hydrogen bonding contacts between the molecule and the peptide in solution due to the *o*-dihydroxy groups from the catechol moiety, resulting in favorable interaction indicated by the large, negative  $\Delta H$  value.<sup>37</sup> The compound **2**, which has a catechol group in the B ring but has no functionality on the A ring, presented a similar result to **4**, indicating that these molecules interact with A $\beta$  similarly due to the presence of the catechol group which facilitates mainly hydrophilic contacts. Despite distinctive, direct contacts predicted with the peptide for **1** compared to **2** and **4**, each of these molecules have favorable Gibbs free energy values that could be used to rationalize their ability to interact with metal-free A $\beta$  species (*vide infra*). The ITC results suggest that **1**, **2**, and **4** bind A $\beta_{40}$ . The mechanism of binding, however, appears to differ with the relative balance of enthalpic and entropic contributions to binding for each compound varying depending on the presence of the catechol group.

Accordingly, the binding of compounds **1** and **4** to A $\beta_{40}$  was subjected to further analysis by NMR. Previously, we have shown that monomeric A $\beta_{40}$  can adopt a  $3_{10}$  helical structure in the central

hydrophobic region at moderate ionic strength and low temperature (PDB ID 2LFM).<sup>38</sup> Using similar conditions, the regions of A $\beta_{40}$  potentially capable of interacting with the aminoisoflavones were mapped. Changes in the SOFAST-HMQC spectra (SOFAST = 2D band-selective optimized flip-angle short transient; HMQC = heteronuclear multiple quantum correlation) of freshly dissolved A $\beta_{40}$  upon titration with **1** and **4** confirmed their potential interaction with three potential peptide sites (Figs. 5 and 6). The chemical shift perturbations were slightly larger for **1** (Figs. 5a and 6b) than **4** (Figs. 5b and 6c), in agreement with the larger free energy change upon binding to A $\beta_{40}$  for compound **1**, as measured by ITC. Moderate (0.02–0.15 ppm on the scaled chemical shift scale) chemical shift perturbations were detected for both compounds in two specific regions of the peptide near the N-terminus (R5–S8) and the N-terminal part of the  $3_{10}$  helix (H13–L17) (Fig. 6a). These two regions are close together in the A $\beta_{40}$  structure (Fig. 6d) and appear to form a potential binding site for the compounds and/or be rearranged upon interaction with the compounds. A third area of chemical shift perturbation is closer to the C-terminus (M35–V40). The chemical shifts near the C-terminus may reflect either the rearrangement of the disordered C-terminus to pack against the aminoisoflavone or may be an indication of a second lower affinity binding site. The perturbation of the chemical shifts on specific residues of A $\beta_{40}$  by aminoisoflavones was notably different than

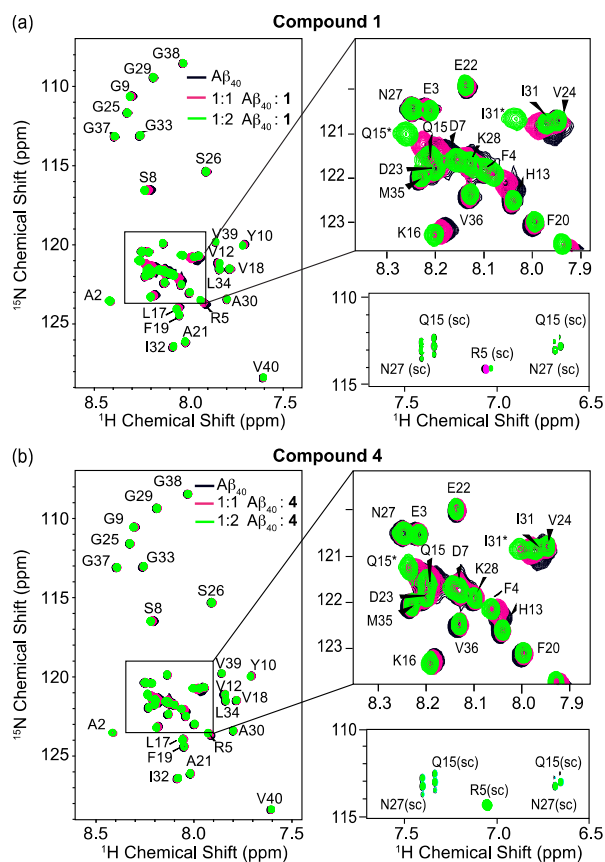


**Fig. 5.** Interaction of **1** and **4** with freshly dissolved A $\beta_{40}$  at near stoichiometric ratios. SOFAST-HMQC spectra of 80  $\mu\text{M}$  freshly dissolved A $\beta_{40}$  in 20 mM deuterated Tris (pH 7.4) with 50 mM NaCl and 10% D $_2$ O and titrated with (a) **1** and (b) **4** to the indicated molar ratios at 4  $^{\circ}\text{C}$ . Chemical shift perturbations were detected primarily for the amide resonances R5–S8 and H13–L17 (see Fig. 6).

what was observed with the related catechol EGCG with A $\beta$ <sub>40</sub> and  $\alpha$ -synuclein, where large nearly uniform decreases in intensity have been observed, suggesting non-specific binding,<sup>12b,14,39</sup> and indicates that polyphenols do not have a single uniform mechanism of binding.<sup>23</sup>

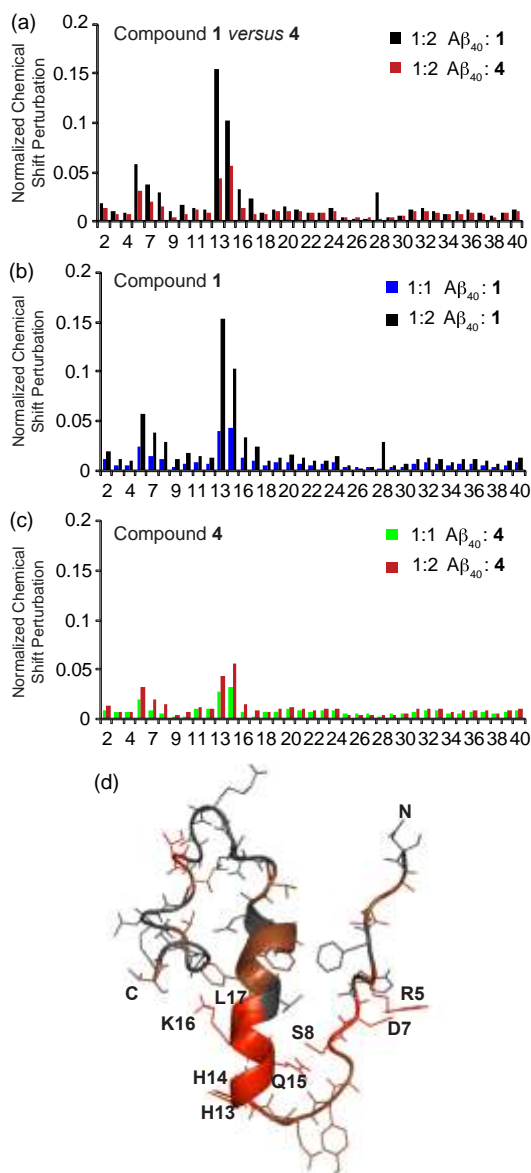


**Fig. 6.** Chemical shift changes in A $\beta$ <sub>40</sub> induced by **1** and **4** (Fig. 5). (a) Chemical shift perturbations for A $\beta$ <sub>40</sub> in the presence of **1** or **4** (1:2 molar ratio). The normalized chemical shift perturbation is equivalent to  $\sqrt{(\Delta^1H)^2 + \frac{(\Delta^{15N})^2}{5}}$ . Normalized chemical shift perturbations for (b) **1** and (c) **4**. (d) Residues with the largest chemical shift perturbations mapped onto the NMR structure of A $\beta$ <sub>40</sub> (PDB 2LFM). The residues with the largest chemical shift perturbations (> 0.02 ppm) are indicated in red, residues with smaller chemical shift perturbations (0.01-0.02 ppm) are presented in brown.

To visualize the potential contacts of **1**, **2**, and **4** with A $\beta$ <sub>40</sub>, flexible ligand docking studies were employed with the solution NMR structure of metal-free A $\beta$ <sub>40</sub> (PDB 2LFM) (Fig. S7).<sup>38</sup> The docked poses of these ligands with the peptide were generally found

in similar positions around the peptide, situated nearer to the N-terminus or 3<sub>10</sub>-helix, similar to the chemical shift perturbations observed by NMR and similar to previous results obtained with the structurally related catechin, EGCG.<sup>12b</sup> Interaction near the N-terminus of A $\beta$ <sub>40</sub> is desirable because the residues that bind Cu(II) and Zn(II) exist in this portion of the sequence, while interaction with the helical portion of the peptide could be beneficial to hinder the initial stages of the self-association region (L17-A21).<sup>1b-e</sup>

The similarity in the pattern of the chemical shift perturbations suggests that **1** and **4** bind to the same site in A $\beta$ <sub>40</sub> (Fig. 6). Although the compounds also often preferred similar binding modes in the docking studies, there were some slight deviations among the results that could support the findings from ITC. For example, there were a few instances where **4** was oriented in a more favourable position to facilitate hydrogen bonding contacts while in some poses, **1** was more aligned with the helical portion of the peptide. Compound **2** could dock in similar positions as both ligands, as expected based on its structure, with most poses being situated near the N-terminus in the area preceding the helical portion of the peptide, similar to the NMR results for **1**. Although the overall view of the ligand interactions with A $\beta$ <sub>40</sub> from NMR and docking are relatively consistent with the ITC results, the magnitude of the interactions cannot be completely determined from either technique. As noted above, only moderate chemical shift perturbations were detected for specific regions of A $\beta$ <sub>40</sub> at 1:1 and 1:2 protein-to-ligand molar ratios. At higher concentrations of compound **1** (1:5 A $\beta$ <sub>40</sub>:**1**), much larger changes in chemical shift were observed along with a strong reduction in intensity (Fig. 7). The changes in chemical shift did not appear to match the pattern obtained at lower concentrations of **1**, although for many residues a definite assignment could not be made. Two new negative (folded) broad peaks were also apparent in the SOFAST-HMQC spectra in the side-chain region of the spectra below 7.5 ppm. The appearance of a new species at higher ligand concentrations was also supported by a strong new peak at 7.64 ppm and three weaker doublets at 6.77, 6.83, and 6.89 ppm in the <sup>1</sup>H spectrum of the ligand (Fig. S8). The intensity changes were not accompanied by the increase in linewidth that would be expected for exchange broadening, suggesting that some of the peptide was lost instead to aggregation. The dramatic changes in the SOFAST-HMQC spectra suggest that either a global conformational change favoring aggregation may have taken place, or compound **1** may have covalently attached to the peptide through Schiff base formation as has been observed before with other flavonoids.<sup>40</sup>

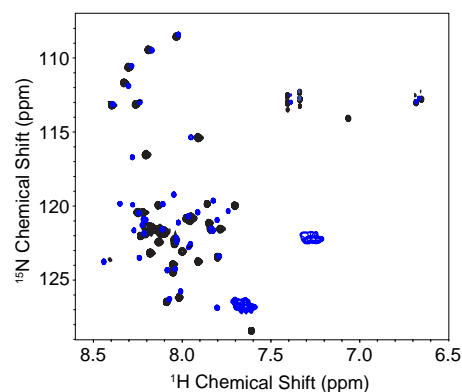


**Fig. 7.** Interaction of A $\beta$ <sub>40</sub> with 5 equiv of **1**. SOFAST-HMQC spectra of 80  $\mu$ M freshly dissolved A $\beta$ <sub>40</sub> (black) in 20 mM deuterated Tris (pH 7.4) with 50 mM NaCl and 10% D<sub>2</sub>O with 5 equiv of **1** (blue) at 4 °C. Large chemical shift changes indicate that a global change in conformation has taken place, possibly due to the formation of covalent adducts.



In addition to binding to freshly dissolved A $\beta$ <sub>40</sub>, compounds **1** and **4** may have the capability to bind to other forms of A $\beta$ <sub>40</sub>, such as fibrils. To probe these possible interactions, we employed saturation transfer difference (STD) NMR experiments to map the regions of the ligand which bind preformed fibrils of A $\beta$ <sub>40</sub> (Fig. 8)<sup>12p,41</sup> and to visualize the potential contacts of **4** with A $\beta$  fibrils, flexible ligand docking studies were employed with the solid state NMR structure of metal-free A $\beta$ <sub>40</sub> (PDB 2LMN and 2LMO) (Figs. 8c, S9, and S10).<sup>42</sup> The normalized signal strengths (STD/STD reference) corresponding to each ligand atom are proportional to its proximity to the amyloid fibril, allowing an atomic-level map of the binding interactions from the ligand to the A $\beta$  fibril to be made.<sup>12p,41</sup> The results from the STD NMR experiments indicate that both **1** and **4** interact fairly strongly (mM to  $\mu$ M dissociation constant) with the fibril to elicit a relatively strong STD signal (approximately 4.5% (for **1**) and 5.9% (for **4**) of the reference signal at a 3 sec saturation power of 50 dB, similar in magnitude to previous results with other catechols<sup>41</sup>). The STD results also suggest that **1** and **4** bind similarly to the A $\beta$  fibril (Fig. 8b).

The STD effect was distributed relatively evenly throughout both compounds, implying that the entire molecule could be packed to some degree against the fibril. In both compounds the strongest interaction is at carbon 8 on the A ring, suggesting the ketone is pointed away from the fibril in both compounds. While the STD pattern was overall similar, carbon 2' in the B ring in **4** was shown to have a significantly higher STD effect than the corresponding carbon in **1**. The increase in this region is an indication that the presence of the catechol group causes a reorientation of **4** to put the B ring in closer contact with the fibril, which may explain the somewhat higher affinity of **4** over **1** for the A $\beta$  fibril. This binding mode is supported and visualized by simulated poses of **4** toward A $\beta$  fibers (PDB 2LMO and 2LMN).<sup>42</sup> In consistent with result from STD NMR, the lowest energy conformation (Fig. 8c) predicted that ring A and B are close to two residues of D23 from adjacent single  $\beta$  strands. These residues were posed within effective hydrogen bonding distance from hydroxyl moieties of **4**, and their potential hydrogen bonding may stabilize this pose. In addition, the aromatic ring A and B were docked to face two hydrophobic I32 residues. Furthermore, the amino group was toward the loop motif which is solvent accessible region. Well fitted conformation of **4** intervening into  $\beta$  sheets around loop region will allow effective hydrogen bonding and hydrophobic interaction with some residues of peptides.

**Antioxidant Properties.** The Trolox antioxidant equivalence capacity (TEAC) assay<sup>43</sup> was conducted to investigate the radical scavenging capability of our aminoisoflavones (Fig. S11).<sup>44</sup> Compared to the vitamin E analogue Trolox, **3** was approximately three times more effective to quench the radical (ABTS<sup>•+</sup>). Compounds **2** and **4** could also reduce the amount of the radical in solution to a similar extent as Trolox. Among the aminoisoflavones, **1** showed the lowest TEAC value suggesting its limited utility as a radical scavenger. Structurally, the most likely radical scavengers among these molecules contain the catechol moiety and may be able to support the resulting ligand intermediate (*e.g.*, semiquinone) upon donation of a hydrogen atom to the organic radical; the absence of the catechol moiety in **1** may preclude its formation of a stable intermediate upon interacting with ABTS<sup>•+</sup>.<sup>44a</sup> To account for their lower TEAC values compared to that of **3**, the possibility for resonance stabilization of **2** and **4** might make them less capable of hydrogen atom donation; the Cl atom in **3** may be capable of producing a radical that could also quench the ABTS<sup>•+</sup>.<sup>44a</sup>

## Conclusions

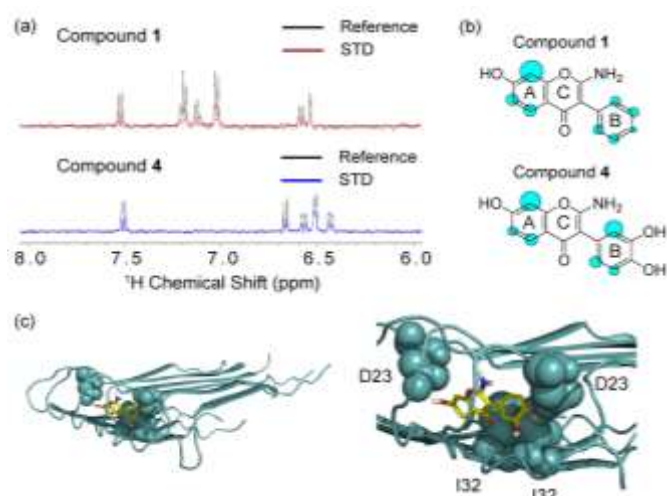


**Fig. 8.** Interaction of **1** and **4** with A $\beta$ <sub>40</sub> fibrils by STD NMR. (a) STD NMR spectra of **1** and **4** at 10:1 ligand to peptide ratio using preassembled A $\beta$ <sub>40</sub> fibrils. A comparison of STD signal intensity to the STD reference reflects the relative proximity of the corresponding proton to the A $\beta$ <sub>40</sub> fibril. (b) Normalized STD intensities mapped onto each compound's structure. Larger blue circles indicate a more intense STD effect. Note that the hydroxyl and amine protons were not detected by this experiment. (c) Docked conformation of **4** to the A $\beta$ <sub>40</sub> fiber (PDB 2LMO)<sup>42</sup> with the lowest energy (right: an expanded view of **4**'s binding site). Residues within effective hydrogen bonding distance from **4** were indicated as spheres. Other docked conformations and corresponding energies are summarized in Figs. S9 and S10.

Advancement in the AD research field has been challenged by the lack of cohesive evidence to explain the origins of the disease. It has been suggested that the formerly competing hypotheses (*i.e.*, metal ion and amyloid cascade) are intertwined. In order to target these two potential pathological factors, efforts have been made to investigate molecules with multiple functions (*i.e.*, metal chelation, A $\beta$  interaction) in hopes of devising a comprehensive structure-interaction-reactivity relationship to govern designs of new chemical tools and/or therapeutics. For this purpose, the flavonoid framework has been identified as a potential avenue, as multiple flavonoids inherently have structural components for interacting with metal ions and A $\beta$ .<sup>12a,12b</sup> In the present study, the flavonoid framework was successfully applied to a synthetic design strategy to generate the aminoisoflavones (*i.e.*, **1-4**). Previous work has shown that flavonoid derivatives, designed with slight modification of the parent natural product framework, led to significant impact upon reactivity (*i.e.*, no reactivity observed)<sup>10</sup>; aminoisoflavones reported herein demonstrated reactivity, even with alterations upon the flavonoid base scaffold. The inclusion of the catechol group with the unnatural primary amine was shown to impart noticeable properties for interaction and reactivity with metals, A $\beta$ , and/or metal-A $\beta$  (*i.e.*, metal chelation, hydrophilic and hydrophobic contacts with A $\beta$  peptides) while additional functional groups (*i.e.*, OH, Cl) did not significantly perturb these properties. This suggests that the catechol moiety may be required to achieve a balance in interaction with metal ions and/or A $\beta$  to influence A $\beta$  aggregation in the absence and presence of metal ions. Furthermore, the catechol moiety was shown to be possibly important for interaction between ligands and metal-A $\beta$  species. In addition, the catechol group also seems to offer other potentially useful properties, such as radical scavenging activity. Thus, this work demonstrates that the flavonoids can be

manipulated into simple structures to tune chemical properties (*i.e.*, metal binding, A $\beta$  interaction) and, subsequently, *in vitro* reactivity toward metal-free and metal–A $\beta$  aggregation, which offers preliminary insights on a structure–interaction–reactivity relationship for flavonoid structures with A $\beta$  and metal–A $\beta$  species.

## Acknowledgements

This work was supported by the Ministero dell'Università e della Ricerca PRIN2010-2011, Prot. No. 20105YY2HL\_006 (to S.M.) and PRIN2010-2011, Prot. no. 20105YY2HL\_002 (to G.B.), the National Institutes of Health (GM-084018) (to A.R.), and the Ruth K. Broad Biomedical Foundation, the National Science Foundation (CHE-1253155), the DGIST R&D Program of the Ministry of Science, ICT and Future Planning of Korea (14-BD-0403), and the 2013 Research Fund (Project Number 1.130068.01) of UNIST (Ulsan National Institute of Science and Technology) (to M.H.L.). D.L. acknowledges support from the Basic Science program through the National Research Foundation of Korea funded by the Ministry of Education, Science, and Technology (2009-0087836). A.S.D. is grateful to the National Science Foundation for a Graduate Research Fellowship. A.K. thanks the Department of Chemistry at the University of Michigan for a Research Excellence Fellowship. We acknowledge Michael Beck for assistance with docking studies.

## Notes and references

<sup>1</sup>Department of Chemistry, University of Michigan, Ann Arbor, Michigan 48109-1055, USA

<sup>2</sup>Biophysics, University of Michigan, Ann Arbor, Michigan 48109-1055, USA

<sup>3</sup>Life Sciences Institute, University of Michigan, Ann Arbor, Michigan 48109-2216, USA

<sup>4</sup>Department of Fine Chemistry, Seoul National University of Science and Technology, Seoul, Korea

<sup>5</sup>Department of Chemistry, Ulsan National Institute of Science and Technology (UNIST), Ulsan 689-798, Korea

<sup>6</sup>Department of Life Sciences and Biotechnology, University of Ferrara, I-44121 Ferrara, Italy

<sup>7</sup>Department of Life and Environment Sciences, Pharmaceutical, Pharmacological and Nutraceutical Sciences Unit, University of Cagliari, I-09124 Cagliari, Italy

<sup>8</sup> These authors contributed equally.

\* To whom correspondence should be addressed: [mhlim@unist.ac.kr](mailto:mhlim@unist.ac.kr), [ramamoor@umich.edu](mailto:ramamoor@umich.edu), and [bbg@unife.it](mailto:bbg@unife.it)

† Electronic Supplementary Information (ESI) available: Table S1 and Figs. S1-S11 are available in the ESI. See DOI: 10.1039/b000000x/

- (a) Alzheimer's Association, *Alzheimers Dement.* 2012, **8**, 131-168. (b) A. S. DeToma, S. Salamekh, A. Ramamoorthy, M. H. Lim, *Chem. Soc. Rev.* 2012, **41**, 608-621. (c) A. S. Pithadia, M. H. Lim, *Curr. Opin. Chem. Biol.* 2012, **16**, 67-73. (d) M. G. Savelieff, S. Lee, Y. Liu, M. H. Lim, *ACS Chem. Biol.* 2013, **8**, 856-865. (e) K. P. Kepp, *Chem. Rev.* 2012, **112**, 5193-5239.
- (a) C. Soto, *Nat. Rev. Neurosci.* 2003, **4**, 49-60. (b) D. B. Teplow, N. D. Lazo, G. Bitan, S. Bernstein, T. Wyttanbach, M. T. Bowers, A. Baumketner, J.-E. Shea, B. Urbanc, L. Cruz, J. Borreguero, H. E. Stanley, *Acc. Chem. Res.* 2006, **39**, 635-645. (c) A. Rauk, *Chem. Soc. Rev.* 2009, **38**, 2698-2715.
- (a) J. Hardy, D. J. Selkoe, *Science* 2002, **297**, 353-356. (b) R. Jakob-Roetne, H. Jacobsen, *Angew. Chem. Int. Ed.* 2009, **48**, 3030-3059. (c) S. Ayton, P. Lei, A. I. Bush, *Free Radic Biol Med* 2013, **62**, 76-89.
- (a) C. A. Ross, M. A. Poirier, *Nat. Med.* 2004, **10 Suppl**, S10-17. (b) M. Fandrich, *Cell. Mol. Life Sci.* 2007, **64**, 2066-2078.
- (a) X. Zhu, B. Su, X. Wang, M. A. Smith, G. Perry, *Cell. Mol. Life Sci.* 2007, **64**, 2202-2210. (b) P. Faller, C. Hureau, *Chem. Eur. J.* 2012, **18**, 15910-15920. (c) M. A. Greenough, J. Camakaris, A. I. Bush, *Neurochem. Int.* 2013, **62**, 540-555. (d) G. Eskici, P. H. Axelsen, *Biochemistry* 2012, **51**, 6289-6311. (e) P. Faller, C. Hureau, *Dalton Trans.* 2009, 1080-1094. (f) P. Faller, *ChemBioChem* 2009, **10**, 2837-2845.
- A. I. Bush, *J. Alzheimers Dis.* 2013, **33 Suppl 1**, S277-S281.
- (a) J. Shearer, V. A. Szalai, *J. Am. Chem. Soc.* 2008, **130**, 17826-17835. (b) J. Shearer, P. E. Callan, T. Tran, V. A. Szalai, *Chem. Commun.* 2010, **46**, 9137-9139. (c) C. Ghosh, S. G. Dey, *Inorg. Chem.* 2013, **52**, 1318-1327. (d) F. Bousejra-ElGarah, C. Bijani, Y. Coppel, P. Faller, C. Hureau, *Inorg. Chem.* 2011, **50**, 9024-9030.
- (a) C. J. Sarell, S. R. Wilkinson, J. H. Viles, *J. Biol. Chem.* 2010, **285**, 41533-41540. (b) D. Noy, I. Solomonov, O. Sinkevich, T. Arad, K. Kjaer, I. Sagi, *J. Am. Chem. Soc.* 2008, **130**, 1376-1383.
- P. Faller, *Free Radic. Biol. Med.* 2012, **52**, 747-748.
- (a) C. Rodríguez-Rodríguez, M. Telpoukhovskaia, C. Orvig, *Coord. Chem. Rev.* 2012, **256**, 2308-2332. (b) J. J. Braymer, A. S. DeToma, J.-S. Choi, K. S. Ko, M. H. Lim, *Int. J. Alzheimers Dis.* 2011, 623051. (c) C. Hureau, I. Sasaki, E. Gras, P. Faller, *ChemBioChem* 2010, **11**, 950-953. (d) A. Dedeoglu, K. Cormier, S. Payton, K. A. Tseitlin, J. N. Kremsky, L. Lai, X. Li, R. D. Moir, R. E. Tanzi, A. I. Bush, N. W. Kowall, J. T. Rogers, X. Huang, *Exp. Gerontol.* 2004, **39**, 1641-1649. (e) W.-h. Wu, P. Lei, Q. Liu, J. Hu, A. P. Gunn, M.-s. Chen, W.-f. Rui, X.-y. Su, Z.-p. Xie, Y.-F. Zhao, A. I. Bush, Y.-m. Li, *J. Biol. Chem.* 2008, **283**, 31657-31664. (f) C. Rodríguez-Rodríguez, N. Sánchez de Groot, A. Rimola, Á. Álvarez-Larena, V. Lloveras, J. Vidal-Gancedo, S. Ventura, J. Vendrell, M. Sodupe, P. González-Duarte, *J. Am. Chem. Soc.* 2009, **131**, 1436-1451. (g) S. S. Hindo, A. M. Mancino, J. J. Braymer, Y. Liu, S. Vivekanandan, A. Ramamoorthy, M. H. Lim, *J. Am. Chem. Soc.* 2009, **131**, 16663-16665. (h) J.-S. Choi, J. J. Braymer, R. P. R. Nanga, A. Ramamoorthy, M. H. Lim, *Proc. Natl. Acad. Sci. U. S. A.* 2010, **107**, 21990-21995. (i) J.-S. Choi, J. J. Braymer, S. K. Park, S. Mustafa, J. Chae, M. H. Lim, *Metallicomics* 2011, **3**, 284-291. (j) J. J. Braymer, J.-S. Choi, A. S. DeToma, C. Wang, K. Nam, J. W. Kampf, A. Ramamoorthy, M. H. Lim, *Inorg. Chem.* 2011, **50**, 10724-10734. (k) A. S. Pithadia, A. Kochi, M. T. Soper, M. W. Beck, Y. Liu, S. Lee, A. S. DeToma, B. T. Ruotolo, M. H. Lim, *Inorg. Chem.* 2012, **51**, 12959-12967. (l) X. He, H. M. Park, S. J. Hyung, A. S. DeToma, C. Kim, B. T. Ruotolo, M. H. Lim, *Dalton Trans.* 2012, **41**, 6558-6566. (m) A. K. Sharma, S. T. Pavlova, J. Kim, D. Finkelstein, N. J. Hawco, N. P. Rath, J. Kim, L. M. Mirica, *J. Am. Chem. Soc.* 2012, **134**, 6625-6636. (n) M. R. Jones, E. L. Service, J. R. Thompson, M. C. P. Wang, I. J. Kimsey, A. S. DeToma, A. Ramamoorthy, M. H. Lim, T. Storr, *Metallicomics* 2012, **4**, 910-920. (o) Y. Liu, A. Kochi, A. S. Pithadia, S. Lee, Y. Nam, M. W. Beck, X. He, D. Lee, M. H. Lim, *Inorg. Chem.* 2013, **52**, 8121-8130. (p) S. Lee, X. Zheng, J. Krishnamoorthy, M. G. Savelieff, H. M. Park, J. R. Brender, J. H. Kim, J. S. Derrick, A. Kochi, H. J. Lee, C. Kim, A. Ramamoorthy, M. T. Bowers, M. H. Lim, *J. Am. Chem. Soc.* 2014, **136**, 299-310.
- (a) M. Ono, M. Haratake, H. Saji, M. Nakayama, *Bioorg. Med. Chem.* 2008, **16**, 6867-6872. (b) M. Ono, Y. Maya, M. Haratake, M. Nakayama, *Bioorg. Med. Chem.* 2007, **15**, 444-450. (c) M. Ono, M. Hori, M. Haratake, T. Tomiyama, H. Mori, M. Nakayama, *Bioorg. Med. Chem.* 2007, **15**, 6388-6396. (d) M. Ono, R. Watanabe, H. Kawashima, T. Kawai, H. Watanabe, M. Haratake, H. Saji, M. Nakayama, *Bioorg. Med. Chem.* 2009, **17**, 2069-2076. (e) H. F. Kung, C. W. Lee, Z. P. Zhuang, M. P. Kung, C. Hou, K. Plossl, *J. Am. Chem. Soc.* 2001, **123**, 12740-12741. (f) W. Zhang, S. Oya, M. P. Kung, C. Hou, D. L. Maier, H. F. Kung, *J. Med. Chem.* 2005, **48**, 5980-5988. (g) M.-P. Kung, C. Hou, Z.-P. Zhuang, B. Zhang, D. Skovronsky, J. Q. Trojanowski, V. M.-Y. Lee, H. F. Kung, *Brain Res.* 2002, **956**, 202-210. (h) W. E. Klunk, Y. Wang, G. F. Huang, M. L. Debnath, D. P. Holt, C. A. Mathis, *Life Sci.* 2001, **69**, 1471-1484. (i) M. Ono, H. Watanabe, R. Watanabe, M. Haratake, M. Nakayama, H. Saji, *Bioorg. Med. Chem. Lett.* 2011, **21**, 117-120.
- (a) A. S. DeToma, J.-S. Choi, J. J. Braymer, M. H. Lim, *ChemBioChem* 2011, **12**, 1198-1201. (b) S.-J. Hyung, A. S. DeToma, J. R. Brender, S. Lee, S. Vivekanandan, A. Kochi, J.-S. Choi, A. Ramamoorthy, B. T. Ruotolo, M. H. Lim, *Proc. Natl. Acad. Sci. U. S. A.* 2013, **110**, 3743-3748. (c) W. M. Tay, G. F. da Silva, L. J. Ming, *Inorg. Chem.* 2013, **52**, 679-690.
- (a) B. H. Havsteen, *Pharmacol. Ther.* 2002, **96**, 67-202. (b) L. H. Yao, Y. M. Jiang, J. Shi, F. A. Tomas-Barberan, N. Datta, R. Singanusong, S. S. Chen, *Plant Foods Hum. Nutr.* 2004, **59**, 113-122. (c) J. Kim, H. J. Lee, K. W. Lee, *J. Neurochem.* 2010, **112**, 1415-1430.

- 14 D. E. Ehrnhoefer, J. Bieschke, A. Boeddrich, M. Herbst, L. Masino, R. Lurz, S. Engemann, A. Pastore, E. E. Wanker, *Nat. Struct. Mol. Biol.* 2008, **15**, 558-566.
- 15 M. Hirohata, K. Ono, J. Takasaki, R. Takahashi, T. Ikeda, A. Morinaga, M. Yamada, *Biochim. Biophys. Acta* 2012, **1822**, 1316-1324.
- 16 (a) E. Middleton, Jr., C. Kandaswami, T. C. Theoharides, *Pharmacol. Rev.* 2000, **52**, 673-751. (b) R. J. Nijveldt, E. van Nood, D. E. C. van Hoorn, P. G. Boelens, K. van Norren, P. A. M. van Leeuwen, *Am. J. Clin. Nutr.* 2001, **74**, 418-425.
- 17 (a) A. E. Martell, R. M. Smith, *Critical Stability Constants*, Plenum, New York, 1974-1989. (b) N. Schweigert, A. J. Zehnder, R. I. Eggen, *Environ. Microbiol.* 2001, **3**, 81-91. (c) A. Avdeef, S. R. Sofen, T. L. Bregante, K. N. Raymond, *J. Am. Chem. Soc.* 1978, **100**, 5362-5370. (d) J. F. Severino, B. A. Goodman, T. G. Reichenauer, K. F. Pirker, *Free Radic Res* 2011, **45**, 115-124. (e) D. R. Eaton, *Inorg. Chem.* 1964, **3**, 1268-1271. (f) W. Kaim, *Dalton Trans.* 2003, 761-768.
- 18 J. McMurry, *Organic Chemistry*, 6th ed., Brooks/Cole--Thomson Learning, Belmont, CA, 2004.
- 19 (a) R. J. Wall, G. He, M. S. Denison, C. Congiu, V. Onnis, A. Fernandes, D. R. Bell, M. Rose, J. C. Rowlands, G. Balboni, I. R. Mellor, *Toxicology* 2012, **297**, 26-33. (b) G. Balboni, C. Congiu, V. Onnis, A. Maresca, A. Scozzafava, J. Y. Winum, A. Maietti, C. T. Supuran, *Bioorg. Med. Chem. Lett.* 2012, **22**, 3063-3066.
- 20 B. G. Jang, S. M. Yun, K. Ahn, J. H. Song, S. A. Jo, Y. Y. Kim, D. K. Kim, M. H. Park, C. Han, Y. H. Koh, *J. Alzheimers Dis.* 2010, **21**, 939-945.
- 21 R. Leuma Yona, S. Mazeres, P. Faller, E. Gras, *ChemMedChem* 2008, **3**, 63-66.
- 22 (a) A. M. Mancino, S. S. Hindo, A. Kochi, M. H. Lim, *Inorg. Chem.* 2009, **48**, 9596-9598. (b) M. T. Soper, A. S. DeToma, S.-J. Hyung, M. H. Lim, B. T. Ruotolo, *Phys. Chem. Chem. Phys.* 2013, **15**, 8952-8961.
- 23 A. R. Ladiwala, J. S. Dordick, P. M. Tessier, *J. Biol. Chem.* 2011, **286**, 3209-3218.
- 24 (a) J. Bieschke, J. Russ, R. P. Friedrich, D. E. Ehrnhoefer, H. Wobst, K. Neugebauer, E. E. Wanker, *Proc. Natl. Acad. Sci. U. S. A.* 2010, **107**, 7710-7715. (b) J. A. Lemkul, D. R. Bevan, *Biochemistry* 2012, **51**, 5990-6009.
- 25 S. Yun, B. Urbanc, L. Cruz, G. Bitan, D. B. Teplow, H. E. Stanley, *Biophys. J.* 2007, **92**, 4064-4077.
- 26 (a) J. J. Braymer, N. M. Merrill, M. H. Lim, *Inorg. Chim. Acta* 2012, **380**, 261-268. (b) T. Storr, M. Merkel, G. X. Song-Zhao, L. E. Scott, D. E. Green, M. L. Bowen, K. H. Thompson, B. O. Patrick, H. J. Schugar, C. Orvig, *J. Am. Chem. Soc.* 2007, **129**, 7453-7463.
- 27 <http://www.acdlabs.com>.
- 28 H. Pajouhesh, G. R. Lenz, *NeuroRx* 2005, **2**, 541-553.
- 29 (a) R. C. Hider, Z. D. Liu, H. H. Khodr, *Methods Enzymol.* 2001, **335**, 190-203. (b) M. Satterfield, J. S. Brodbelt, *Anal. Chem.* 2000, **72**, 5898-5906.
- 30 M. J. Sever, J. J. Wilker, *Dalton Trans.* 2004, 1061-1072.
- 31 C. A. Tyson, A. E. Martell, *J. Am. Chem. Soc.* 1968, **90**, 3379-3386.
- 32 P. Verma, J. Weir, L. Mirica, T. D. Stack, *Inorg. Chem.* 2011, **50**, 9816-9825.
- 33 D. Maity, A. K. Manna, D. Karthigeyan, T. K. Kundu, S. K. Pati, T. Govindaraju, *Chemistry* 2011, **17**, 11152-11161.
- 34 T. Kundu, B. Sarkar, T. K. Mondal, S. M. Mobin, F. A. Urbanos, J. Fiedler, R. Jiménez-Aparicio, W. Kaim, G. K. Lahiri, *Inorg. Chem.* 2011, **50**, 4753-4763.
- 35 J. Balla, T. Kiss, R. F. Jameson, *Inorg. Chem.* 1992, **31**, 58-62.
- 36 J. S. Thompson, J. C. Calabrese, *J. Am. Chem. Soc.* 1986, **108**, 1903-1907.
- 37 S. H. Wang, F. F. Liu, X. Y. Dong, Y. Sun, *J. Phys. Chem. B* 2010, **114**, 11576-11583.
- 38 S. Vivekanandan, J. R. Brender, S. Y. Lee, A. Ramamoorthy, *Biochem. Biophys. Res. Commun.* 2011, **411**, 312-316.
- 39 S. Sinha, Z. Du, P. Maiti, F. G. Klarner, T. Schrader, C. Wang, G. Bitan, *ACS Chem. Neurosci.* 2012, **3**, 451-458.
- 40 (a) N. Popovych, J. R. Brender, R. Soong, S. Vivekanandan, K. Hartman, V. Basur, P. M. Macdonald, A. Ramamoorthy, *J. Phys. Chem. B* 2012, **116**, 3650-3658. (b) M. Zhu, S. Rajamani, J. Kaylor, S. Han, F. Zhou, A. L. Fink, *J. Biol. Chem.* 2004, **279**, 26846-26857. (c) F. L. Palhano, J. Lee, N. P. Grimster, J. W. Kelly, *J. Am. Chem. Soc.* 2013, **135**, 7503-7510.
- 41 C. Airoidi, E. Sironi, C. Dias, F. Marcelo, A. Martins, A. P. Rauter, F. Nicotra, J. Jimenez-Barbero, *Chem. Asian J.* 2013, **8**, 596-602.
- 42 A. T. Petkova, W.-M. Yau, R. Tycko, *Biochemistry* 2006, **45**, 498-512.
- 43 The ABTS<sup>+</sup> radicals employed in the TEAC assay do not represent ROS, such as hydroxyl radicals.
- 44 (a) C. A. Rice-Evans, N. J. Miller, G. Paganga, *Free Radical Biol. Med.* 1996, **20**, 933-956. (b) R. Re, N. Pellegrini, A. Proteggente, A. Pannala, M. Yang, C. Rice-Evans, *Free Radic. Biol. Med.* 1999, **26**, 1231-1237.